# The long-term carbon cycle, fossil fuels and atmospheric composition

Robert A. Berner

Department of Geology and Geophysics, Yale University, New Haven, Connecticut 06520-8109, USA (e-mail: robert.berner@yale.edu)

The long-term carbon cycle operates over millions of years and involves the exchange of carbon between rocks and the Earth's surface. There are many complex feedback pathways between carbon burial, nutrient cycling, atmospheric carbon dioxide and oxygen, and climate. New calculations of carbon fluxes during the Phanerozoic eon (the past 550 million years) illustrate how the long-term carbon cycle has affected the burial of organic matter and fossil-fuel formation, as well as the evolution of atmospheric composition.

The carbon cycle is a variety of processes that take place over timescales ranging from hours to millions of years. Processes occurring over shorter periods include photosynthesis, respiration, air–sea exchange of carbon dioxide and humus accumulation in soils. However, it is the long-term carbon cycle, occurring over millions of years, that is of interest when considering the origin of fossil fuels. The long-term cycle, shown in Fig. 1, is distinguished by the exchange of carbon between rocks and the surficial system, which consists of the ocean, atmosphere, biosphere and soils. The long-term carbon cycle is the main controller of the concentration of atmospheric carbon dioxide and (along with the sulphur cycle) atmospheric oxygen over a geological timescale[1,2]. It can be represented succinctly by the generalized reactions[3,4]:

$$CO_2 + CaSiO_3 \leftrightarrow CaCO_3 + SiO_2 \qquad (1)$$

$$CO_2 + H_2O \leftrightarrow CH_2O + O_2 \qquad (2)$$
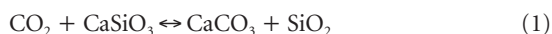
These reactions summarize many intermediate steps. Equation (1), going from left to right, represents the uptake of atmospheric carbon dioxide during the weathering on land of calcium (and magnesium) silicates, with the dissolved weathering products (Ca^{2+}, Mg^{2+} and HCO_3^-) delivered to the ocean and precipitated there as calcium and magnesium carbonates in sediments. Going from right to left, equation (1) represents the deep burial and thermal decomposition of carbonates with the liberated carbon dioxide released into the atmosphere and oceans.

Equation (2) is of particular interest for this review. Going from left to right, it represents net global photosynthesis (photosynthesis minus respiration), as manifested by the burial of organic matter (CH_2O) in sediments. The buried organic matter is eventually transformed, mostly to kerogen, but some becomes oil, gas and coal. Equation (2), going from right to left, represents the oxidative weathering of organic matter exposed by erosion on the continents (and to a lesser extent the combination of thermal decomposition of organic matter to reduced gases with consequent oxidation of the gases in the atmosphere). The burning of fossil fuels by humans has caused a large increase in the rate of organic matter oxidation compared with that of the natural weathering process. This increase, on the basis of the data we present in this review and that of the IPCC[5], is an acceleration by a factor of about 100. Thus, humans have greatly perturbed the long-term carbon cycle.

This review shows that numerical modelling, based on the long-term carbon cycle, allows the calculation of global rates of organic matter burial over geological time, and that the resulting rate distribution bears a resemblance to times of formation of oil and gas source rocks and coal. In addition, the complex feedbacks that govern organic burial are shown to be intimately tied to oceanic nutrients, the carbon dioxide and oxygen content of the atmosphere, and climate.
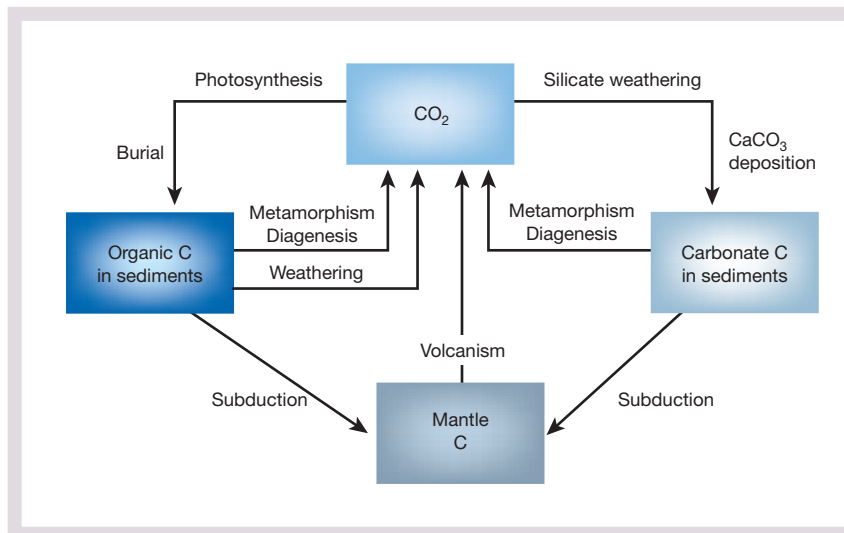
Figure 1 A model of the long-term carbon cycle. The deposition of carbonates derived from the weathering of carbonates is not shown because these processes essentially balance one another over the long term as far as carbon dioxide is concerned. However, carbonate deposition derived from carbonate weathering leads to additional degassing of carbon dioxide upon deep burial and thermal decomposition. Diagenesis, chemical changes at low temperatures during burial. The cycle can be subdivided into two subcycles involving organic matter (left side of figure) and silicate weathering and carbonate deposition (right side of figure).

Organic matter burial and source rocks

There are two principal methods for estimating the global rate of burial of organic matter over a geological timescale. The first involves determining the mean concentration of organic carbon in sedimentary rocks and correcting for the loss of the volume of rocks with time owing to erosion, metamorphism (transformation by natural agencies such as heat and pressure) and subduction (the sideways and downwards movement of plates of the Earth's oceanic crust)[6]. The second, reported here, is based on the use of the carbon isotopic composition of seawater. During photosynthesis ^{12}C is taken up preferentially instead of ^{13}C, such that the organic matter derived from organisms is about 20‰ lower in ^{13}C than the carbon in atmospheric carbon dioxide or that in dissolved inorganic carbon (DIC) of sea water. A compilation of $\delta^{13}C$ of carbonate fossils versus time has been performed[7] (where $\delta^{13}C(‰) = [(^{13}C/^{12}C_{sample})/(^{13}C/^{12}C_{standard})-1]1,000$). Changes in $\delta^{13}C$ of carbonates with time are assumed to record the average $\delta^{13}C$ value for DIC in sea water and also for atmospheric carbon dioxide (which is about 7‰ lower in ^{13}C than DIC). The rate of preferential removal from the ocean and atmosphere of isotopically light organic carbon, relative to total carbon, is recorded by the value

of $\delta^{13}C$. For example, an increase in $\delta^{13}C$ for sea water normally represents increased removal of light carbon and, thus, greater burial of organic matter in sediments. By performing mass-balance calculations for both total carbon and ^{13}C for input and output of carbon to the oceans plus the atmosphere, it is possible, by using the $\delta^{13}C$ isotopic data, to calculate the global rate of burial, over time, of organic carbon in sediments, both of marine and non-marine origin[2,8–11].

A plot of global organic burial rate during the Phanerozoic eon is shown in Fig. 2, and the pattern is a crude guide to the occurrence of fossil-fuel source rocks, as will be seen later. The burial curve is calculated using variable isotope fractionation during photosynthesis[11,12], new data on $\delta^{13}C$ for the late Permian period[13] and data on the rapid recycling of carbon in younger rocks[6,11]. The estimated error is ±50% of the rate plotted. The most prominent feature is a broad maximum centred around 300 Myr ago (Permo-Carboniferous period). This maximum is a direct consequence of the very high $\delta^{13}C$ of the ocean and atmosphere at this time[7]. Prominent minima occur before ~470 Myr ago (early Paleozoic era) and around 220–180 Myr ago (Triassic–Early Jurassic period), whereas secondary maxima are at 440–410 Myr ago (Silurian period) and 90–120 Myr ago (Middle Cretaceous period).

The times of maximum model-calculated organic carbon burial coincide with independent estimates of the times of major oil source rock deposition. The relative areas of the six principal source-rock periods[14] expressed as a percentage of the total for all areas coincide in time with the maxima in the calculated carbon burial curve (Fig. 2). Also, the minima in the carbon-burial curve coincide with periods of very low occurrence of source rocks for oil and coal[14,15]. This agreement suggests that a major factor in oil generation is increased global deposition of organic matter.

Klemme and Ulmishek[14] have divided their six source-rock periods into two categories, source rocks dominated by type I and type II kerogen (sedimentary organic matter that is high in hydrogen and low in oxygen derived mainly from aquatic planktonic organisms), and those dominated by type III kerogen (lower in hydrogen, higher in oxygen and derived mainly from plants), with coal included with type III as a source rock (mainly for gas). The ratio of type III kerogen to total kerogen for each period is plotted in Fig. 3. The broad maximum centred about 300 Myr ago illustrates the importance of coal deposition at that time. The rise of land plants between 380 and 350 Myr ago during the Devonian period created a new source of relatively non-biodegradable organic matter, lignin, which, when buried in sediments, gave rise to increased global burial of organic carbon in the Carboniferous and Permian (350–250 Myr ago) (Fig. 2). Burial of lignin and other plant products gave rise to the great Permian and Carboniferous coal basins and, to a lesser extent, type III kerogen for oil and gas formation. By far the most abundant coal reserves are from the Permo-Carboniferous period[15], even though these older rocks have been subjected to erosion for longer times than younger deposits. Other periods of high type III kerogen formation (Fig. 3) are the Middle Cretaceous (90–120 Myr ago) and mid-Tertiary (30–50 Myr ago). These are also periods of abundant coal deposition[15]. It is notable that the time when both global organic burial and source rock deposition were at their lowest (centred around 200 Myr ago in Fig. 2) is also the time when very little coal was deposited[15].

The temporal distribution of the different kerogen types correlates somewhat with the loci of organic matter deposition over time. The latter can be estimated by means of isotope mass-balance modelling for both carbon and sulphur[8]. This is because of the different sulphur content, which is mainly found in pyrite (FeS_2), of organic-rich sediments deposited in different sedimentary environments. The global rate of burial of sedimentary pyrite can be calculated, in a manner analogous to that used for the burial of organic matter. The sulphur isotopic composition of sea water, as recorded in deposits of gypsum and anhydrite and traces of sulphate in carbonates[16], generally reflect changes in the rate of preferential removal of ^{32}S from sea water as pyrite. Pyrite is lower in $^{34}S/^{32}S$ relative to seawater sulphate,
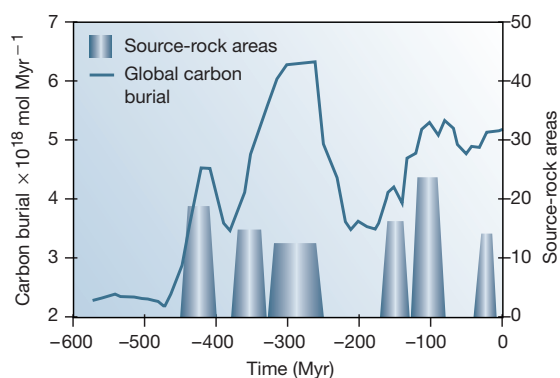
Figure 2 Plot of global organic carbon burial during the Phanerozoic eon compared with the times of deposition of major oil and gas source rocks. (Carbon burial rate modified from ref. 11; source-rock areas from ref. 14.) Units for source-rock area are in percentages of the total of the six areas. Source-rock abundances at other times are very minor[14]. The very high carbon burial values centred around 300 Myr ago are due predominantly to terrestrial carbon burial and coal formation[8].
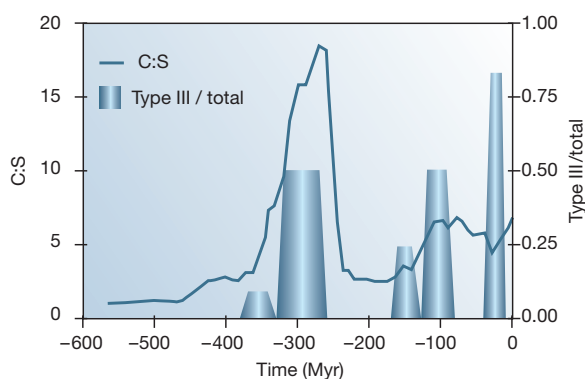
Figure 3 Plots of organic carbon/pyrite sulphur (C:S) buried in sediments versus time, compared with the fraction of oil and gas source rocks that are of type III (including coal). (C:S values from ref. 11; source rock data from ref. 14).

because the reduction of sulphate to H$_2$S, from which pyrite forms, involves a large isotopic fractionation[16]. Sulphur isotopic data for the ocean, combined with mass-balance calculations for total sulphur and ^{34}S, enable the calculation of rates of pyrite burial over time.

Ratios of the burial rates of organic carbon and pyrite sulphur (C:S) versus time are also shown in Fig. 3. The changes with time of C:S agree with what is known about pyrite formation in modern sediments[8]. Predominant burial in organic-rich marine sediments, for instance in basins with anoxic bottom water such as the Black Sea, involves abundant sulphate reduction and pyrite formation, leading to low C:S ratios. Burial in fresh-water environments, such as coal swamps, results in very high C:S ratios. This is because of the very low sulphate content of fresh water compared with that of sea water, which minimizes pyrite formation[8]. (Burial in oxygenated marine bottom waters with bioturbation results in intermediate C:S values, but this environment is not as favourable for oil formation[17]). Thus, for oil-prone marine source rocks deposited under anoxic bottom-water conditions[17], one would expect low C:S ratios, and for coal deposits, one would expect high C:S ratios. The correlation between type III kerogen, relative to total kerogen, and C:S ratio (Fig. 3) agrees with this prediction for several source-rock periods (Fig. 3).

The very low values of C:S for the early Paleozoic (before 370 Myr ago) suggest greater deposition in unusually organic-rich and pyrite-rich marine rocks. This is in agreement with the widespread occurrence of the graptolite black shale facies of this era, which has been interpreted to have been deposited in abundant anoxic regions of the ocean[18]. (The very low C:S values also reflect the relative lack of deposition in fresh water, owing to the absence of large land plants at that time.) The argument that there is little difference in organic preservation between oxygenated and non-oxygenated bottom waters[19] is controversial and does not agree with other studies of modern sediments or with geological observations[17,20,21].

The presence of only a moderately high proportion of type III kerogen in Permo-Carboniferous source rocks, compared with the very high concurrent values of C:S, may be because the compilation of Klemme and Ulmishek[14] was oriented towards oil and gas formation, not coal abundance. Also, the poor correlation between the ratio of type III to total kerogen and C:S for the mid-Tertiary (40–20 Myr ago) is explained by the deposition of much terrestrially derived (type III) organic matter in marine estuarine and deltaic environments[14], where abundant pyrite formation is supported by sulphate-rich sea water.

## Organic burial, nutrients and atmospheric composition

The burial of organic matter, as it affects source-rock formation, is intimately tied to the chemical composition of the oceans and atmosphere. For the atmosphere, as shown by equation (2), the burial of organic matter involves the removal of carbon dioxide and the addition of oxygen. In this way, organic burial, on a geological timescale, is a major controller of atmospheric composition. Atmospheric composition, in turn, exerts a major control on organic matter burial and acts in a feedback capacity. A major factor linking organic burial in the marine environment and atmospheric composition is the level of essential nutrients in sea water, principally phosphorus and nitrogen[22]. This is because biological production is normally limited by nutrients. Changes in atmospheric carbon dioxide and oxygen can affect the availability of nutrients, which in turn affect organic production and burial. This leads to a variety of biogeochemical feedbacks that control both atmospheric composition and organic burial. Because of this complex web of feedbacks, a simple explanation of the various changes over time in rates of organic burial and source-rock formation (Figs 2 and 3) is difficult, with the exception of the effect of the rise of large land plants on terrestrial carbon burial.

The interaction of nutrients and atmospheric carbon dioxide and oxygen with organic burial can be represented by systems-analysis diagrams. An example is shown in Fig. 4. (A complete coverage of all suggested linkages is beyond the scope of this review — for more
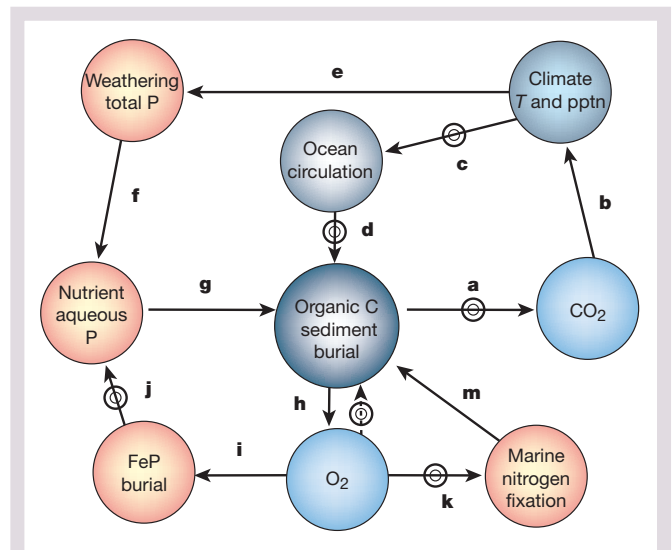
Figure 4 Systems-analysis diagram showing some of the feedback relationships between marine organic carbon burial, nutrients, climate, atmospheric carbon dioxide and oxygen, and ocean circulation. The upward dashed arrow at **h** represents disagreement concerning the effect of oxygen on organic burial. (See text for detailed explanation). Solid arrows represent positive responses and arrows with bullseyes represent negative responses. A loop with an even number of arrows with bullseyes, or with no bullseyes, represents a positive feedback loop. A loop with an odd number of bullseyes represents negative feedback. FeP, phosphorus associated with ferric oxide.

details consult refs 23–25.) Plain arrows between entities represent positive responses. This means, for example, if organic burial increases, oxygen production and, therefore oxygen level, increases. Arrows with attached bullseyes refer to negative responses. For example, if organic burial increases, carbon dioxide (the ultimate source of the carbon) decreases. By following the diagram, one can deduce whether various loops lead to positive or negative feedback. A loop with an even number of arrows with bullseyes or no bullseyes represents positive feedback. A loop with an odd number of bullseyes represents negative feedback. Because atmospheric oxygen and carbon dioxide have not varied considerably over geological timescales, interest has focused on negative feedback pathways, which provide stabilization.
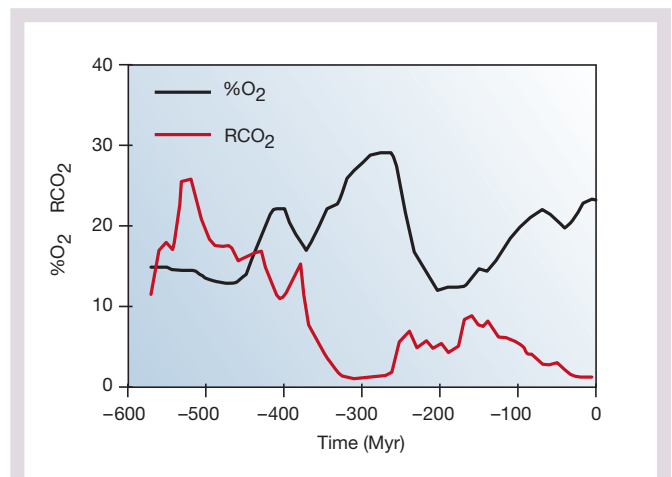
Figure 5 Plots of RCO$_2$ (the ratio of the mass of carbon dioxide in the atmosphere in the past to that for the pre-industrial present) and %O$_2$ during the Phanerozoic eon. (Values of RCO$_2$ from the GEOCARB III model[33]; values of %O$_2$ from ref. 11 using the ^{13}C data of refs 12 and 13). Estimated errors are ±50% for RCO$_2$ and ±7% for O$_2$.

It is instructive to follow several of the loops shown in Fig. 4. Consider the loop h–i–j–g. Increased organic burial raises atmospheric oxygen, which results in a more oxygenated ocean and the greater burial of phosphorus associated with ferric oxides (FeP). Burial of FeP robs the ocean of available dissolved phosphorus for photosynthesis, resulting in a lower mean phosphorus concentration, and this results in lowered biological productivity and less organic burial. This negative feedback loop is thought to be a major stabilizing control on atmospheric oxygen over a geological timescale[26,27]. An alternative suggestion is that nitrogen fixation is the primary factor limiting organic production[28]. In this case, loop h–k–m provides the negative feedback; greater organic burial produces higher oxygen, and this inhibits biological nitrogen fixation, which means lower nitrogen levels in sea water and lower organic production and burial.

Atmospheric carbon dioxide is also involved in negative feedback with regard to organic carbon burial. Consider the loop a–b–c–d. Greater burial leads to a lowering of atmospheric carbon dioxide, which, because of the atmospheric greenhouse effect, leads to global cooling, especially at high latitudes[29]. A cooler Earth with a greater latitudinal temperature gradient could drive greater oceanic circulation and a greater supply of oxygen to deep waters. This inhibits the formation of anoxic bottom waters and thereby reduces organic burial[17]. This loop has three arrows with bullseyes, and this indicates overall negative feedback. (An additional scenario is that greater oceanic circulation could lead to a greater supply of nutrients to surface waters with greater organic production, greater burial and positive feedback). Finally, there is the loop a–b–e–f–g. Higher organic burial causes lower carbon dioxide and a cooler Earth, which reduces the rate of weathering on land of rocks containing phosphorus. This means less delivery of phosphorus to the oceans, lower marine-dissolved phosphorus, and lower biological production and organic burial[30,31]. Other possible negative-feedback loops have been suggested, such as greater organic burial, elevated oxygen, reduced plant-assisted weathering of phosphate minerals, less phosphorus transport to the sea and lower organic carbon burial[23].

The arrow going from oxygen to organic matter is dashed. This is because there is controversy over whether the oxygen content of the atmosphere and oceans has a direct influence on global organic matter burial. Studies of the modern ocean[20,21] suggest that organic matter preservation in sediments is considerably reduced by the presence of oxygen in bottom waters, but a simple inverse correlation between measurable oxygen level and organic matter burial has not been found[32]. Also, high concentrations of organic matter can be found in oxygenated bottom waters under zones of high plankton productivity[19].

Using a large variety of feedback mechanisms (many of which are not illustrated in Fig. 4), concentrations of carbon dioxide and oxygen in the atmosphere over a geological timescale have been calculated by computer modelling[6,11,31,33–36]. A review of these models and their results can be found in ref. 25. An example based on modelling, by myself, of a variety of processes[11,33], including calcium and magnesium silicate and carbonate weathering and burial, organic matter weathering and burial, pyrite weathering and burial, and global CO_2 degassing, is shown in Fig. 5. (From sensitivity analysis, the errors in carbon dioxide are about ±50% and for oxygen about ±7% oxygen.) A variety of independent estimates agree with the curve for carbon dioxide[37,38], and biological data agree with elevated Permo-Carboniferous oxygen levels[24]. The most prominent feature in these plots are the high oxygen levels and low carbon dioxide levels during the Permo-Carboniferous. These are due primarily to the rise of large vascular land plants and their effect on accelerated silicate weathering (for carbon dioxide) and increased organic matter burial (for both carbon dioxide and oxygen).

Modelling of the long-term carbon cycle can lead to new insights regarding the formation of source beds for oil, coal and gas and the relationship between global organic matter burial and the composition of the atmosphere. Futher work is needed to better identify the principal feedback relations and to better quantify the various fluxes within the carbon cycle. □

1. Garrels, R. M., Lerman, A. & Mackenzie, F. T. Controls of atmospheric O₂ and CO₂ — past, present, and future. *Am. Sci.* **64,** 306–315 (1976).
2. Holland, H. D. *The Chemistry of the Atmosphere and Oceans* (Wiley, New York, 1978).
3. Ebelmen J. J. Sur les produits de la décomposition des espèces minérales de la famille des silicates. *Annu. Rev. Mines* 12, 627–654 (1845).
4. Urey, H. C. *The Planets: their Origin and Development* (Yale Univ., New Haven, 1952).
5. IPCC (Intergovernmental Panel on Climate Change) *Climate Change 2001: Synthesis Report* (IPCC, Geneva, 2001).
6. Berner, R. A. & Canfield, D. E. A model for atmospheric oxygen over Phanerozoic time. *Am. J. Sci.* **289,** 333–361 (1989).
7. Veizer, J. *et al.* ⁸⁷Sr/⁸⁶Sr, δ¹³C and δ¹⁸O evolution of Phanerozoic seawater. *Chem. Geol.* **161,** 59–88 (1999).
8. Berner, R .A. & Raiswell, R. Burial of organic carbon and pyrite sulfur in sediments over Phanerozoic time: a new theory. *Geochim. Cosmochim. Acta* **47,** 855–862 (1983).
9. Garrels R. M. & Lerman, A. Coupling of the sedimentary sulfur and carbon cycles – an improved model. *Am. J. Sci.* **284,** 989–1007 (1984).
10. Walker J. C. G. Global geochemical cycles of atmospheric oxygen. *Mar. Geol.* **70,** 159–174 (1986).
11. Berner, R. A. Modeling atmospheric O₂ over Phanerozoic time. *Geochim. Cosmochim. Acta* **65,** 685–691 (2001).
12. Hayes, J. M, Strauss, H. & Kaufman, A. J. The abundance of ¹³C in marine organic matter and isotope fractionation in the global biogeochemical cycle of carbon during the past 800 Ma. *Chem. Geol.* **161,** 103–125 (1999).
13. Korte, C, Kozur, H. W., Joachimski, M. M. & Veizer, J. Strontium, oxygen and carbon isotope records of Permian seawater. *Eur. Geophys. Soc. Geophys. Res. Abstr.* **5,** 13061 (2003).
14. Klemme, H. D. & Ulmishek, G. F. Effective petroleum source rocks of the world: stratigraphic distribution and controlling depositional factors. *Bull. Am. Ass. Petrol. Geol.* **75,** 1809–1851 (1991).
15. Bestougeff, M. A. Summary of world coal resources and reserves. *26th Int. Geol. Cong. Paris Colloq.* **35,** 353–366 (1980).
16. Strauss, H. Geological evolution from isotope proxy signals — sulfur. *Chem. Geol.* **161,** 89–101 (1999).
17. Demaison, G. J. & Moore, G. T. Anoxic environments and oil source bed genesis. *Bull. Am. Ass. Petrol. Geol.* **64,** 1179–1209 (1980).
18. Berry, W. B. N. & Wilde, P. Progressive ventilation of the oceans — an explanation for the distribution of the lower Paleozoic black shales. *Am. J. Sci.* **278,** 257–275 (1978).
19. Pederson, T. F. & Calvert, S. E. Anoxia vs productivity: what controls the formation of organic carbon-rich sediments and sedimentary rocks. *Bull. Am. Ass. Petrol. Geol.* **74,** 454–466 (1990).
20. Canfield, D. E. Factors influencing organic carbon preservation in marine sediments. *Chem. Geol.* **114,** 315–329 (1994).
21. Hedges J. I. *et al.* Sedimentary organic matter preservation: A test for selective degradation under oxic conditions. *Am. J. Sci.* **299,** 529–555 (1999).
22. Falkowski, P. G. & Raven, J. *Aquatic Photosynthesis* (Blackwell, Oxford, 1997).
23. Lenton T. M. & Watson, A. J. Redfield revisited 2: What regulates the oxygen content of the atmosphere? *Glob. Biogeochem. Cycles* **14,** 249–268 (2000).
24. Berner, R. A., Beerling, D. J., Dudley, R., Robinson, J. M. & Wildman, R. A. Phanerozoic atmospheric oxygen. *Annu. Rev. Earth Planet. Sci.* **31,** 105–134 (2003).
25. Berner, R. A. *The Phanerozoic Carbon Cycle* (Oxford Univ. Press, Oxford, in the press).
26. Van Cappellen, P. & Ingall, E. D. Redox stabilization of the atmosphere and oceans by phosphorus-limited marine productivity. *Science* **271,** 493–496 (1996).
27. Colman, A. S. & Holland, H. D. *Marine Authigenesis: From Microbial to Global* (eds Glenn, C., Lucas, J. & Prevot-Lucas, L.) 53–75 (Soc. Econ. Paleontologists & Mineralogists, 2000).
28. Falkowski, P. G. Evolution of the nitrogen cycle and its influence on the biological sequestration of CO₂ in the ocean. *Nature* **387,** 272–275 (1997).
29. Crowley, T. J. & North, G. R. *Paleoclimatology* (Oxford Univ. Press, Oxford, 1991).
30. Weissert, H. C. Isotope stratigraphy, a monitor of paleoenvironmental change: a case study from the Early Cretaceous. *Surv. Geophys.* **10,** 1–61 (1989).
31. Wallmann, K. Controls on the Cretaceous and Cenozoic evolution of seawater composition, atmospheric CO₂ and climate. *Geochim. Cosmochim. Acta* **65,** 3005–3025 (2001).
32. Betts, J. N. & Holland, H. D. The oxygen content of ocean bottom waters, the burial efficiency of organic-carbon and the regulation of atmospheric oxygen. *Palaeogeogr., Palaeoclimatol., Palaeoecol.* **97,** 5–18 (1991).
33. Berner, R. A. & Kothavala, Z. GEOCARB III: A revised model of atmospheric CO₂ over Phanerozoic time. *Am. J. Sci.* **301,** 182–204 (2001).
34. Hansen, K. W. & Wallmann, K. Cretaceous and Cenozoic evolution of seawater composition, atmospheric O₂ and CO₂. *Am. J. Sci.* **303,** 94–148 (2003).
35. Tajika, E. Climate change during the last 150 million years: reconstruction from a carbon cycle model. *Earth Planet Sci. Lett.* **160,** 695–707 (1998).
36. Bergman, N., Lenton, T. & Watson, A. Coupled Phanerozoic predictions of atmospheric oxygen and carbon dioxide. *Eur. Geophys. Soc. Geophys. Res. Abstr.* **5,** 11208 (2003).
37. Royer, D. L., Berner, R. A. & Beerling, D. J. Phanerozoic atmospheric CO₂ change: evaluating geochemical and paleobiological approaches. *Earth Sci. Rev.* **54,** 349–392 (2001).
38. Crowley, T. J. & Berner, R. A. CO₂ and climate change. *Science* **292,** 870–872 (2001).